



Analysis of Exhaled Human Breaths using Graphene Gas Sensor Based on the Male Gender

Nur Hazah Shamsudin^{1,*}, Siti Amaniah Mohd Chachuli², Calvin Jeffry Jalan¹, Omer Coban³, Nazreen Waeleh², Siti Aisah Mat Junos², Nur Asmiza Selamat¹, Nursabillilah Mohd Ali¹

¹ Fakulti Teknologi dan Kejuruteraan Elektrik, Universiti Teknikal Malaysia Melaka, 76100 Durian Tunggal, Melaka, Malaysia

² Fakulti Teknologi dan Kejuruteraan Elektronik dan Komputer, Universiti Teknikal Malaysia Melaka, 76100 Durian Tunggal, Melaka, Malaysia

³ Engineering Faculty, Ataturk University, 25250 Erzurum, Turkey

ARTICLE INFO

Article history:

Received 27 September 2023

Received in revised form 6 June 2024

Accepted 21 August 2024

Available online 19 September 2024

Keywords:

Graphene; human breath; screen-printing; breath sensor; thick film

ABSTRACT

Breath analysis is an intriguing method that has the potential to significantly improve non-implantable physical health management via the use of flexible sensors to monitor breathing behaviours. In comparison to other analytical techniques for detecting breath elements, non-invasive breathing diagnostics based on chemical sensors can provide numerous benefits, including nanotechnology, power efficiency, simplicity of structure, and cost-effectiveness, contributing to the flexibility of experimental studies. This paper presents the graphene-based human breath sensor. Graphene was prepared in a paste form by mixing the graphene powder with two types of the binder. Two binders were prepared to compare their performance to human breath. The graphene paste was deposited using screen-printing on different substrates, Kapton film, and glass. The sensing film was thermally annealed at 200°C for 30 minutes and characterized using SEM and FTIR. All graphene gas sensor samples responded well to collected male human breath samples: Bumiputera (Sarawak), Malay, Chinese, and Indian. The best graphene gas sensor for males was OG-T(G) and OG-T(K) with sensitivity, $S=1.10415$ and $S=1.01629$. Based on the comparison results of male human breath, the fastest response time and recovery time were 0.52s and 13s, respectively.

1. Introduction

Human breath has long been one of the three major biological media for monitoring human health and environmental exposure, alongside urine and blood. The detection of odor on the human breath, as described by Hippocrates around 400 BC, is regarded as the first analytical health evaluation tool [1-3]. Although less frequent than modern bio-fluid tests, breath sampling has become a popular diagnostic tool since it is non-invasive, allows unlimited timing and volume, and does not require clinical personnel. Breath research has made significant progress in assessing health states during the last two decades, overcoming many early hurdles connected to collection and

* Corresponding author.

E-mail address: nurhazahsha@utem.edu.my

<https://doi.org/10.37934/araset.51.2.190205>

analysis. Exhaled breath is the most approachable biological sample for diagnostic examination since it is emitted spontaneously and in huge quantities. A human inhales and then exhales around 10,000 L of air every day. Exhaled breath contains water vapors and hundreds of various trace compounds of exogenous and endogenous origin in parts per billion (ppb) to parts per million (ppm) levels, except for Nitrogen (N₂) (78.04 %), Oxygen (O₂) (16 %), Carbon Dioxide (CO₂) (4–5 %), and other inert gases [4-6]. Exhaled breath monitoring is an essential topic for researchers that have recently attracted attention due to advancements in analytical techniques and nanotechnology. It is now a non-invasive technique for disease identification, medical monitoring, and metabolic state monitoring that examines the volatile organic compounds (VOCs) in exhaled breath.

Gas chromatography-mass spectrometry (GC-MS) is the current standard for determining and monitoring volatile organic compounds (VOCs) [7,8]. It is the preferred approach for analyzing the qualitative properties of complicated gaseous mixtures. However, it has some constraints, such as the relatively long time required for a single test and the labor-intensive sample preparation. Standard solutions must also be used to execute a quantitative analysis, which not only increases the expense but also has a severe influence on the environment, particularly in the case of screening analysis [9]. A screening analysis is an analytical process that consists of extraction, isolation, and possible identification of a compound or group of compounds in a sample with the minimum number of steps and the minimal manipulation of the sample.

Moreover, human breath analysis with GC-MS requires substantial training from the instrument manufacturer or practitioner with GC-MS competence. Proton transfer reaction mass spectrometry (PTR-MS) is a technology designed particularly for detecting gaseous organic chemicals in breath [10,11]. Contrary to GC-MS, PTR-MS provides relative VOC concentrations with excellent sensitivity without sample isolation and purification. However, such procedures take more extended preparation. The disadvantages of PTR-MS include its inability to discriminate between compounds with the same molecular weight [12]. It necessarily requires the use of a skilled operator, or more specifically, a highly educated person. For example, it is unsuitable for people with diabetes, and the PTR-MS is large and cumbersome, making it unsuitable for routine diabetic monitoring. Selected ion flow tube mass spectrometry (SIFT-MS) is another analytical technique for measuring numerous trace gases in air and breath in real-time. It depends on Hydronium ion (H₃O⁺), Nitrosonium ion (NO⁺), and Dioxygenyl ion (O₂⁺) precursor ions to chemically ionize trace gas molecules in air or breath samples delivered into the helium carrier gas [13,14]. SIFT-MS can identify absolute quantities of trace gases in single-breath exhalation down to ppb levels without sample collection or calibration. Unfortunately, the failure of SIFT-MS as a viable tool for monitoring diseases such as diabetes is due to its incapacity to detect chemicals in a gas mixture [15]. Similar to GC-MS and PTR-MS, SIFT-MS needs the use of a qualified operator to prolong the equipment handling. Another significant and widespread disadvantage is the mobility of the equipment to be mobilized from one place to another.

Graphene has outstanding advantages of a large surface area, excellent conductivity, high mechanical strength, and excellent thermal conductivity [16]. It is also a potential 2D material for numerous applications, particularly in creating sensing and implantable health monitoring devices. Graphene performance diversity allows for the realization of a wide range of applications such as gas sensing [17,18], antimicrobial nano activity [19,20], saturable absorber [21], lubricants [22], and drug delivery applications [23]. Many strategies such as spin-coating, ink-jet printing, screen printing, drop-casting, dip-coating, and sputtering have been widely used to coat graphene on different substrates to fabricate graphene film conductive layers [24]. Graphene-based biochemical sensors outperform conventional carbon electrode-based sensors in terms of sensitivity, limits of detection, and reaction time. Thus, numerous graphene-based biochemical sensors for health monitoring have

been developed, including detecting electrolytes and metabolites in biomarkers and analyzing volatile organic compounds (VOCs) in exhaled breath, such as acetone, ethanol, and ammonia, and other biochemical applications. Graphene has generally been recognized among the most preferred nanostructures for human monitoring and sensing applications. The capability being a carbon allotrope with exceptional sensory properties, is ideal for attaining the best performance in terms of sensitivity, linearity, responsiveness, and recovery durations [25].

In comparison of invasive method, such as GC-MS, PTR-MS and SIFT-MS which necessitate longer and complex data analytical procedures, this paper presents a low-cost, easily processable graphene gas sensor based exhaled breath for breath measurement analysis. The graphene was deposited on different substrates: Kapton film and glass, using the screen-printing method. The graphene gas sensor was exposed to the collected male human breath. The result showed that the proposed graphene gas sensor exhibited a good response to male human breath samples.

2. Experimental Section

2.1 Preparation of Binder and Graphene Paste

There were two types of binder used, namely standard binder and oil binder. The standard binder was prepared by mixing the Ethyl Cellulose (2 wt.%) with α -Terpineol (98 wt.%) until homogeneous. As for the oil, the binder used Ethyl Cellulose (2 wt.%), α -Terpineol (90 wt.%), and Linseed oil (8 wt.%). Both binders underwent magnetic stirring for 24 hours. The graphene paste is also prepared into two types: standard graphene paste and oil graphene paste. Both pastes were prepared by mixing the graphene powder (5 wt.%) and binder (95 wt.%) using magnetic stirring for 24 hours.

2.2 Fabrication of Graphene Gas Sensor

The fabrication of the graphene gas sensor was using the screen-printing deposition method. The size of the sensing layer was set to 1 cm x 1 cm. The sensing materials graphene was deposited onto different substrates, which are Kapton tape and glass. The interdigitated electrode type was used as the electrode, and silver paste was used as the electrode material. There were two (2) positions of electrode applied to the gas sensor, known as 'top' and 'bottom'. Top position refers to the electrode deposition at the first layer on the substrate, while the graphene was deposited onto the second layer. For the bottom electrode, the deposition of electrode was layered at the second layer, and the second layer of the substrate was deposited with graphene layer. Fine copper wires were attached to the leg of the electrode for the electrical flow of the sensor. Sample names for the gas sensor is listed in Table 1. All samples are differed according to the types of binder used in paste preparation, the electrode position and the types of substrate in deposition. SG-T(G) and SG-T(K) are standard binder with first layered graphene on the glass and kapton substrate respectively. Similar binder with second layered of graphene on the glass and kapton substrate signifies as SG-B(G) and SG-B(K) respectively.

Table 1
 Labelling for the graphene gas sensor

Graphene paste	Electrode position	Type of substrate	Sample name
Standard	Bottom	Glass	SG-T(G)
		Kapton	SG-T(K)
	Top	Glass	SG-B(G)
		Kapton	SG-B(K)
Oil	Bottom	Glass	OG-T(G)
		Kapton	OG-T(K)
	Top	Glass	OG-B(G)
		Kapton	OG-B(K)

Contrary to the standard binder, the oil binder is initially denoted as ‘O’. The OG-T(G) indicates oil binder graphene deposition at the first layer of the glass substrate, while OG-T(K) is oil binder graphene deposition at the first layer of the kapton substrate. Whereas, the second layered of graphene deposited onto the glass and kapton substrate are named as OG-B(G) and OG-B(K) respectively. All fabricated graphene gas sensors are shown in Figure 1 for clear image representation.

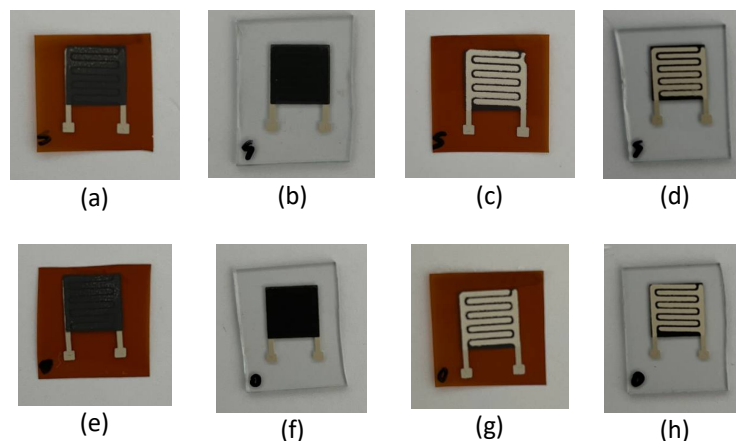


Fig. 1. Fabricated graphene gas sensor (a) SG-T(K), (b) SG-T(G), (c) SG-B(K), (d) SG-B(G), (e) OG-T(K), (f) OG-T(G), (g) OG-B(K), and (h) OG-B(G)

2.3 Measurement of Human Breath Sensor

The experimental setup for the human breath sensor is shown in Figure 2. The human needs to exhale their breath into the Tedlar bag. For analysis of the exhaled human breath pattern towards the graphene gas sensor, the collection of human breath is focused on male samples at the ranging age of 20 to 30 years old, which is obtained from four (4) main ethnicities of Malaysia. The ethnicities are Bumiputera (Sarawak), Malay, Chinese, and Indian. Firstly, the eight (8) samples are exposed to the human breath sample from Bumiputera (Sarawak). Two gas sensors that produced a better result in human breath samples were chosen, and the gas sensor was used for human breath samples from Malay, Chinese, and Indian.

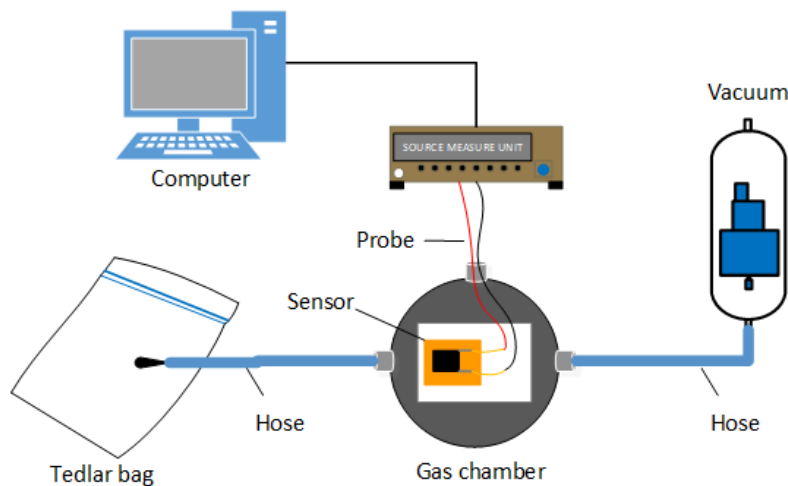


Fig. 2. Experimental setup of human breath sensor

Table 2 shows the four (4) males of human breath samples categorized into Malay, Chinese, Indian, and Bumiputera (Sarawak). Sample M-1 was used as a reference for male models to observe responses from the prepared samples.

Table 2

Man human breath samples

Race	Male	Quantity
Bumiputera (Sarawak)	M-1	1
Malay	M-2	1
Chinese	M-3	1
Indian	M-4	1

The voltage of 1V is supplied to the graphene gas sensor using a Source Measure Unit (SMU) (Keithley 6487). Initially, the gas sensor was kept stable for 300 s. The exhaled human breath was then, released into the gas chamber for 60 s and continually flowed to another 300 s. The continuous flow of exhaled human breath at the aforementioned time is significance, in purpose of achieving its initial value of 300 s for sensor recovery characteristics observation. The response of the human breath sensor was recorded using Labview software.

2.4 Characterization using SEM and FTIR

The sensing layer of the graphene gas sensor was characterized using Scanning Electron Microscope (SEM) and Fourier Transform Infrared Spectroscopy (FTIR). Figure 3 illustrates the SEM morphology view of standard graphene paste and oil graphene paste after annealed treatment.

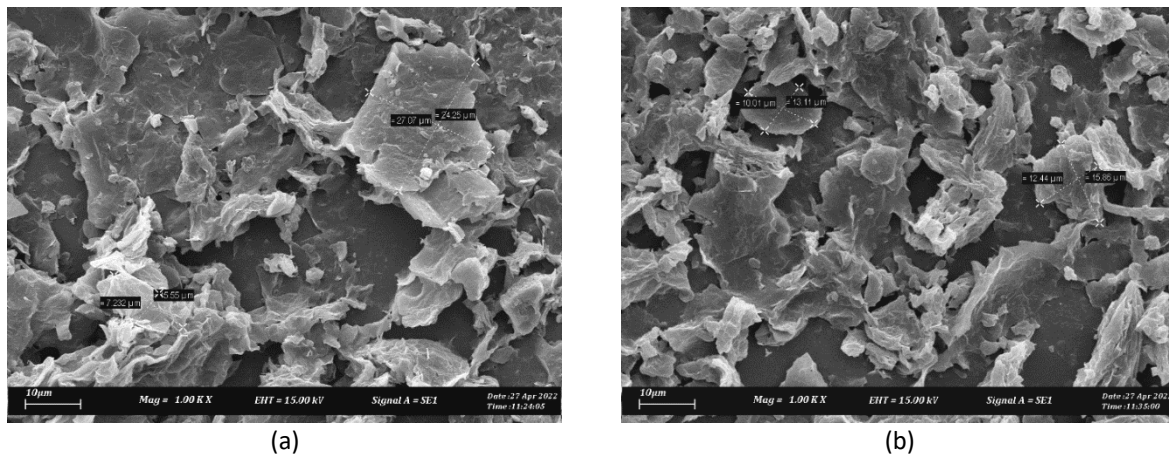


Fig. 3. Morphology of sensing layer after annealed treatment: (a) standard graphene paste and (b) oil graphene paste

Error! Reference source not found. shows the cross-section of the standard graphene paste and oil graphene paste after annealed treatment. It shows that the dimension of the flakes was 10-30 µm. The average thickness shows were 13 - 23 µm.

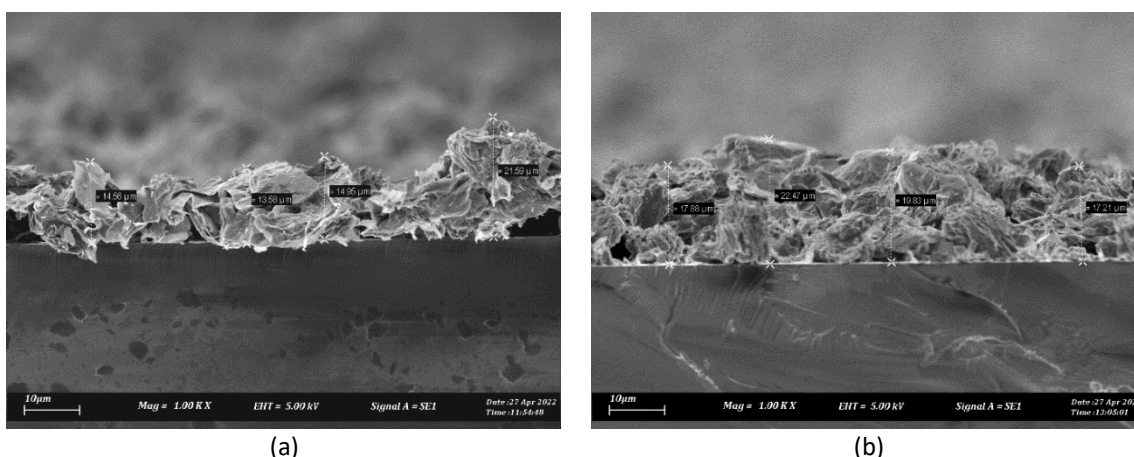


Fig. 4. Cross-section of sensing layer after annealed treatment: (a) standard graphene paste and (b) oil graphene paste

Figure 5 shows the FTIR spectrum of oil graphene paste, oil binder, standard graphene paste, and standard binder. Various oxygen configurations in the structure, which the absorption band at 3745 cm^{-1} was assigned to the O-H group stretching vibrations. As can be seen, O-H was less absorbed in oil graphene paste compared to the others. The absorption peak at 2922 cm^{-1} can be assigned to the C-H stretching of alkane functional groups. The absorption peak at about 1155 cm^{-1} was assigned to the C-F stretching of the fluoro compound, and the absorption peak at 916 cm^{-1} was assigned to the C=C bending of alkene vibrations [26].

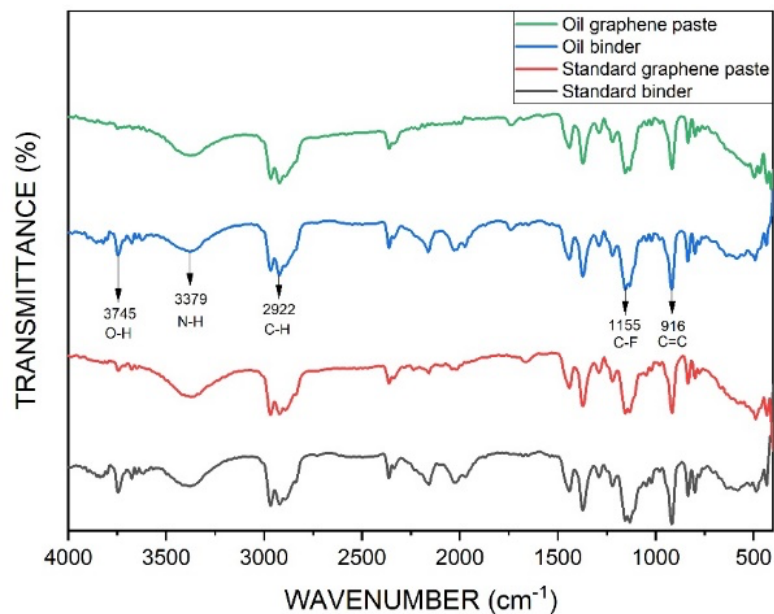


Fig. 5. FTIR spectrum of oil graphene paste, oil binder, standard graphene paste, and standard binder

3. Results and Discussion

3.1 Current-Voltage (IV) Characteristic of Graphene Gas Sensor

Error! Reference source not found. shows the Current-voltage (I–V) characterizations of the graphene sensor conducted at room temperature to examine the ohmic nature during operational circumstances. It is observed that the curves are linear. The resistance of a chemo-resistive sensor varies in response to chemical reactions occurring at its surface, and this change in resistance is recorded by an external circuitry coupled to the sensor through its electrodes [27]. The straight lines in the I–V plot indicate that the connections between the silver electrode and graphene sensing material adhere to Ohm's law, which guarantees effective sensor performance [28,29]. The selected supply voltage for this experiment was 1V.

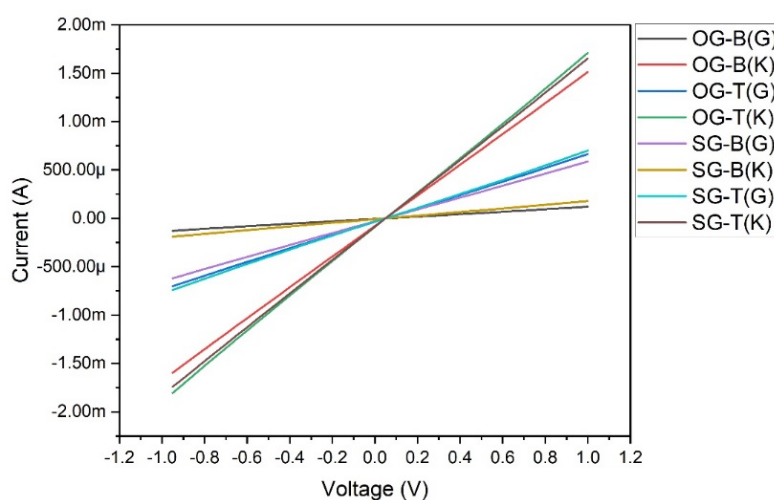


Fig. 6. Graph for graphene gas sensor

Error! Reference source not found. shows the resistance of the graphene gas sensor. The highest resistance reading was 7.649 kΩ for OG-B(G) sample, which this sample was fabricated using Oil

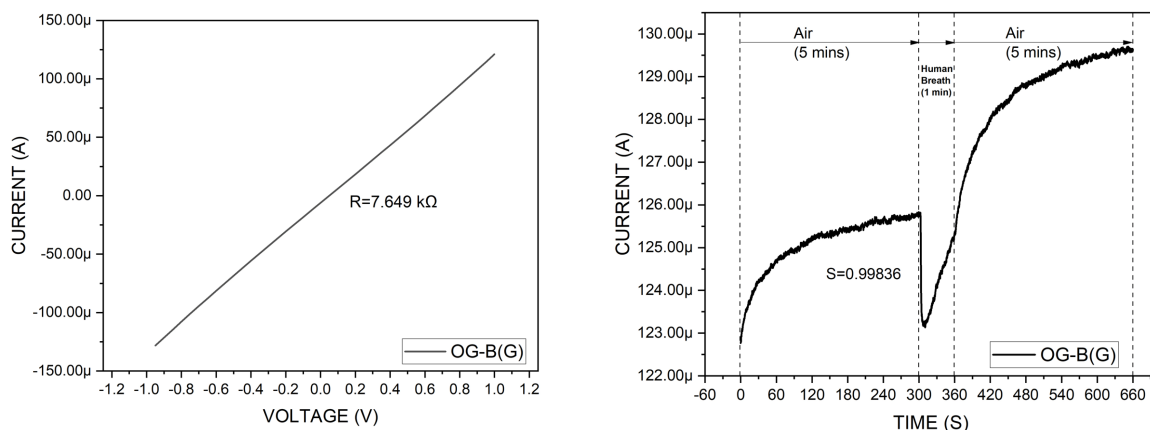
Graphene paste at the bottom and an electrode on top on a glass substrate. As shown, most of the electrodes that were deposited on the top of the sensing material exhibited high resistance, which was OG-B(K) 0.624 kΩ, SG-B(G) 1.605 kΩ, and SG-B(K) 5.250 kΩ. This relates to the heating frequency toward the sample during the fabrication process. Contrary to the bottom layered of electrode which was double heated during the process, the top layered of electrode was heated only once at 150°C for 30 minutes. The double heated of electrode increased its metallic elements and conductivity, thereby reducing the resistivity, if compared to the single heated of top layered of electrode.

Table 3
 Resistance of the graphene gas sensor

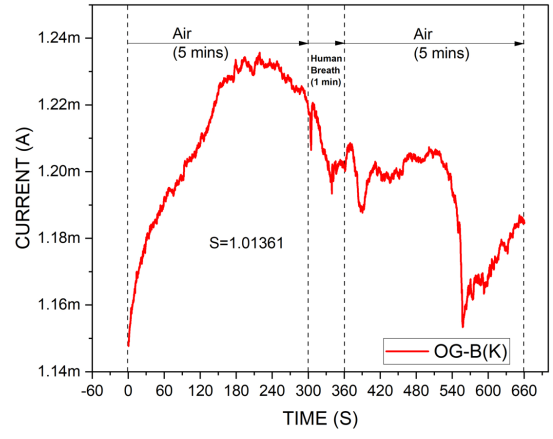
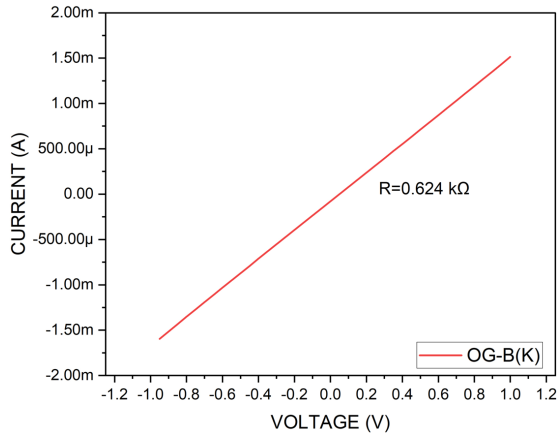
No.	Sensor Samples	Resistance
1	OG-B(G)	7.649 kΩ
2	OG-B(K)	0.624 kΩ
3	OG-T(G)	1.409 kΩ
4	OG-T(K)	0.548 kΩ
5	SG-B(G)	1.605 kΩ
6	SG-B(K)	5.250 kΩ
7	SG-T(G)	1.324 kΩ
8	SG-T(K)	0.570 kΩ

3.2 Response to Male Human Breath Samples

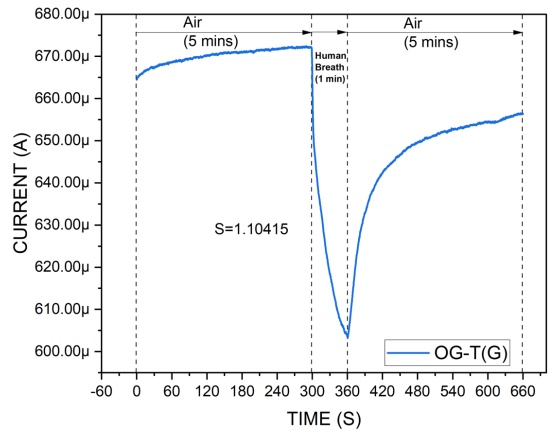
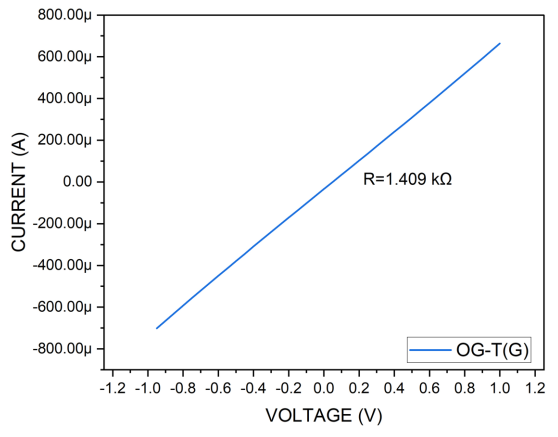
Error! Reference source not found. shows the M-1 human breath response to eight graphene gas sensors. The graph presents the I-V characteristic of the sensor and the response of the gas sensor to the human breath samples. Based on Figure 7(c), the sensor exhibits the highest sensitivity toward human breath with $S=1.10415$. During the first 300 seconds in the presence of air, the sensor shows an average resistance of 1.493 kΩ. Then, the human breath was exposed for 60 seconds, and the average resistance of 1.653 kΩ. The sensor shows a great response to the presence of human breath. The sensor was exposed to the presence of air for another 300 seconds to recover. It shows that the sensor does not recover well during the required time.



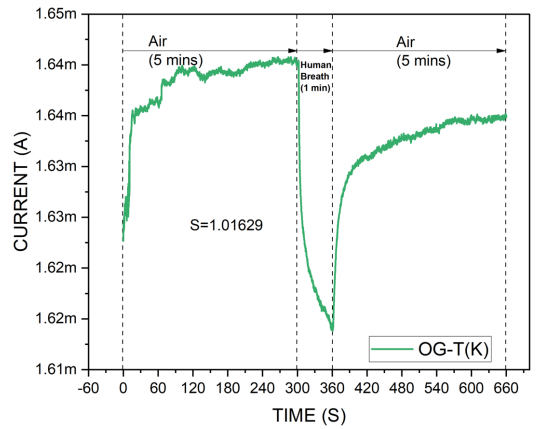
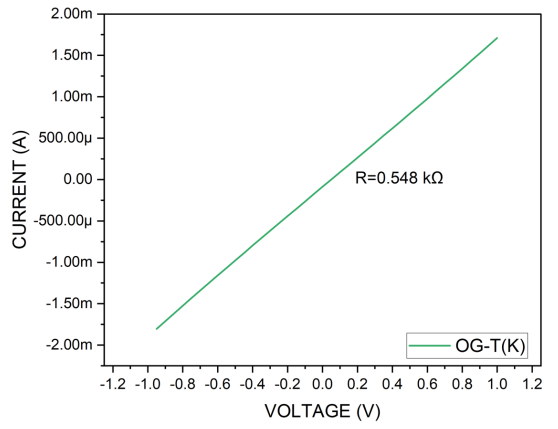
(a)



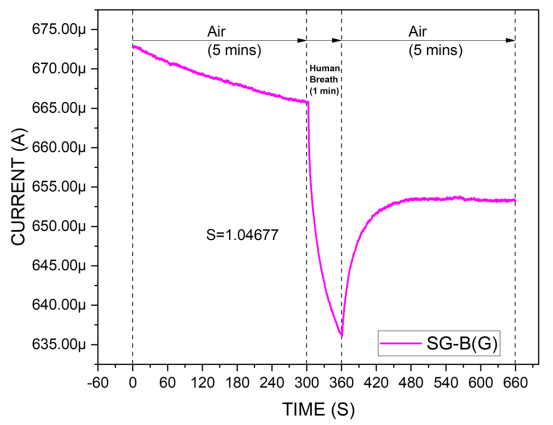
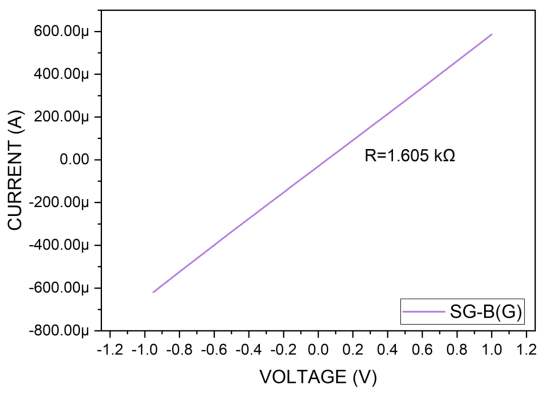
(b)



(c)



(d)



(e)

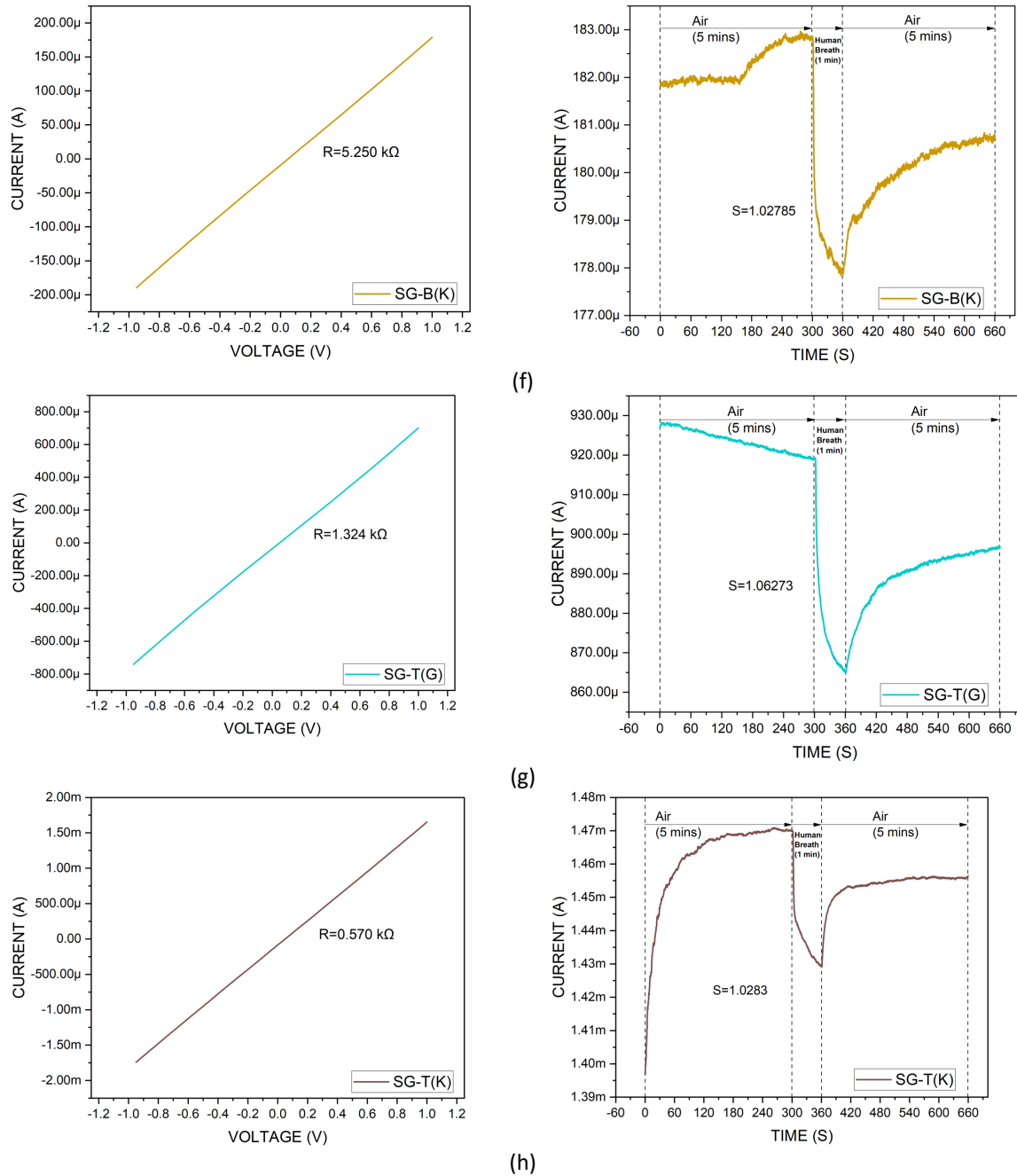


Fig. 7. M-1 human breath response to graphene sensor (a) OG-B(G), (b) OG-B(K), (c) OG-T(G), (d) OG-T(K), (e) SG-B(G), (f) SG-B(K), (g) SG-T(G), and (h) SG-T(K)

Table 4 shows the sensor parameter performance for M-1. The sensitivity, S was calculated as follows;

$$S = \frac{I_a}{I_g} \tag{1}$$

I_a = the current of air

I_g = the current of human breath

The highest sensitivity was produced by SG-T(G), and the lowest was OG-B(G). This result showed that graphene deposited on the top of the electrode generates better sensitivity than graphene deposited on the bottom of the electrode. The graphene deposited on the top enables the sensor to

absorb more human breath, while the graphene deposited at the bottom takes a long distance to reach the sensing area and causes less human breath adsorption, thus less sensitivity.

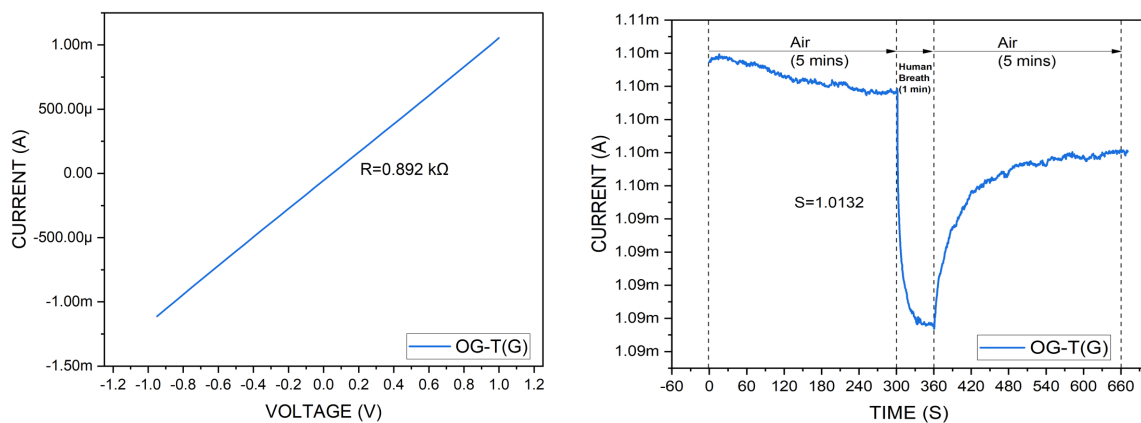
Table 4
 Graphene sensor parameter performances for male

Sample Name	Sensitivity	Response Time	Recovery Time	Recovery Characteristic
OG-B(G)	0.99836	3.86	179	Not recover well
OG-B(K)	1.01361	3.38	297	Not recover well
OG-T(G)	1.10415	0.52	143	Not recover well
OG-T(K)	1.01629	2.51	104	Not recover well
SG-B(G)	1.04677	3.18	51	Not recover well
SG-B(K)	1.02785	1.70	154	Not recover well
SG-T(G)	1.06273	2.52	171	Not recover well
SG-T(K)	1.0283	2.45	73	Not recover well

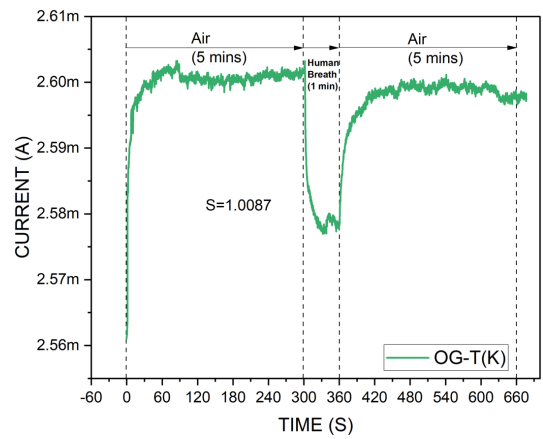
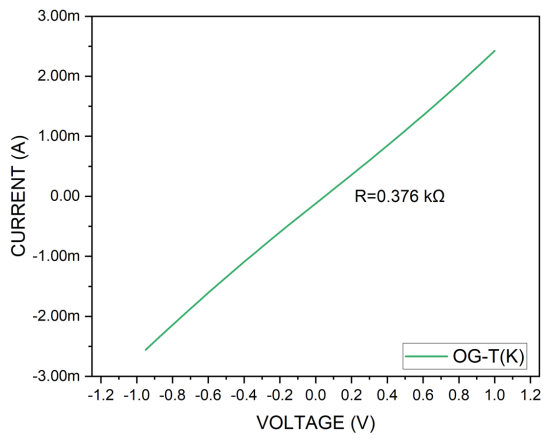
Based on the response and performance exhibited by the gas sensors displayed in Table 4, the selected graphene gas sensor for comparison with others male human breaths were OG-T(G) and OG-T(K). The OG-T(G) showed the highest sensitivity towards human breath with a response time of 0.52s and recovery time of 143s. This result is based on the graphene deposited on the top of the gas sensor. The sensing area on the top also makes the gas sensor adsorb higher human breath, thus producing a faster response time. As for OG-T(K) showed a response time of 2.51s and a recovery time of 104s. Moreover, both sensors displayed stable current compared to the other.

3.3 Comparison with Other Male Human Breath Samples

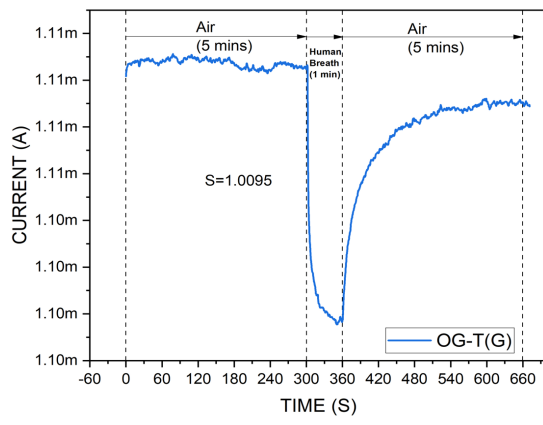
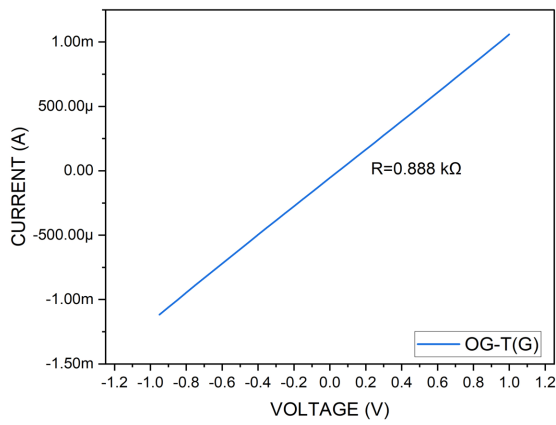
Based on the previous results, the selected graphene gas sensors for males were OG-T(G) and OG-T(K) because of their high sensitivity to human breath. The gas sensor was fabricated anew to avoid the effects of the first human breath. **Error! Reference source not found.** shows the sensor OG-T(G) and OG-T(K) response toward the male human breath M-2, M-3, and M-4.



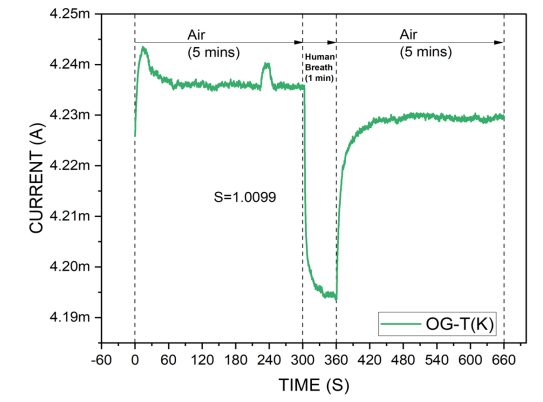
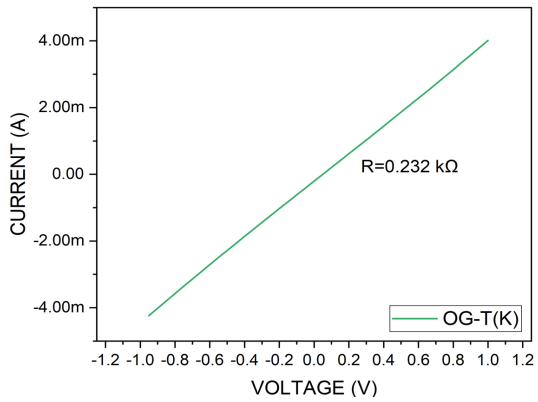
(a)



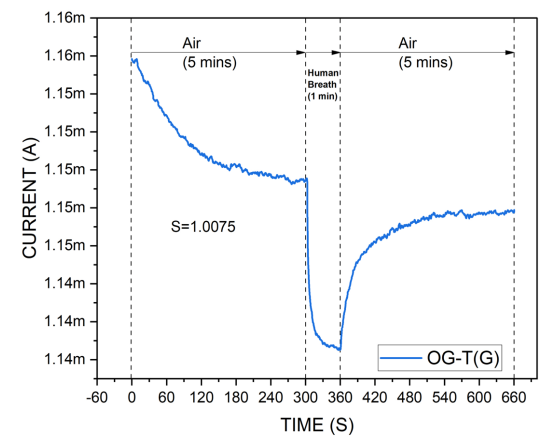
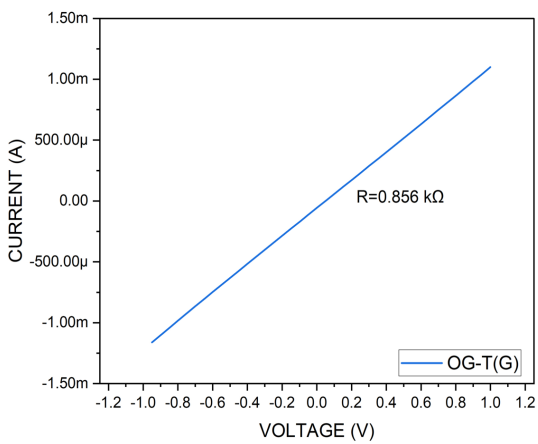
(b)



(c)



(d)



(e)

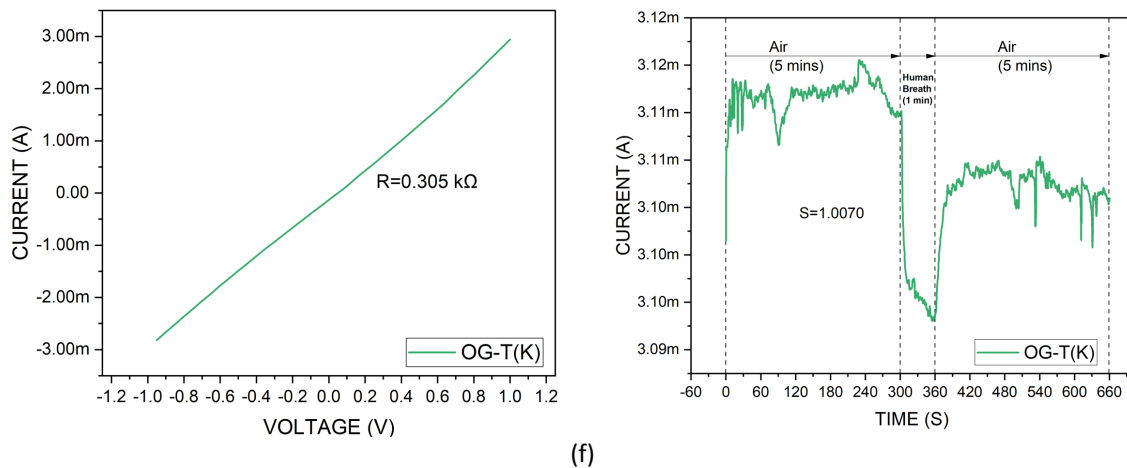


Fig. 8. Response of OG-T(G) and OG-T(K) gas sensors toward other male human breath (a)-(b) M-2, (c)-(d) M-3 and (e)-(f) M-4

Based on the graph pattern shown in **Error! Reference source not found.**, all gas sensors responded to the three male human breaths. Primarily the gas sensor did not achieve the actual value after the human breath was exposed, but only one sensor managed to recover well, which was the male, M-2 OG-T(K). The resistance exhibited by each type of sensor was almost the same. The resistance may be affected by the types of substrate used in this study. Kapton is thermally conductive, which improves its function as an electrically insulating coating between a component and its heating element [30]. As for glass, its optical properties lead to potential applications in the transmission of optical signals, which is becoming increasingly important in high data transmission rate devices [31].

Table 5 shows the comparison of sensors OG-T(G) and OG-T(K) performances for male M-1, M-2, M-3, and M-4 human breath. Based on the comparison outcome, OG-T(G) for human breath (M-1) produced the highest sensitivity, $S=1.10415$, and the response time, 0.52s compared to other samples. The fastest recovery time was sensor OG-T(K) sample human breath M-3 with 13s to achieve a recovery state. Every sample has a different parameter performance. This might be due to the fabrication of the sensor, such as might different concentrations of graphene during the deposition, thus affecting the sensor's active area. Moreover, human breath collected also shows a different sensor response. The results of the gas sensor also can be affected by the individual lifestyle, diet, and mental-emotional state or process [32].

Table 5

Comparison of sensor parameter performance for male human breath

Sample	Sensitivity	Response Time (s)	Recovery Time (s)	Recovery Characteristic
M-1				
OG-T(G)	1.10415	0.52	143	Not recover well
OG-T(K)	1.01629	2.51	104	Not recover well
M-2				
OG-T(G)	1.0132	1.75	127	Not recover well
OG-T(K)	1.0087	2.03	28	Recover well
M-3				
OG-T(G)	1.0095	2.12	140	Not recover well
OG-T(K)	1.0099	3.32	13	Not recover well
M-4				
OG-T(G)	1.0075	3.11	106	Not recover well
OG-T(K)	1.0070	2.85	18	Not recover well

4. Conclusions

In conclusion, the graphene gas sensor for a human breath sensor has been successfully fabricated using the screen-printing method. The graphene gas sensors were fabricated onto Kapton and glass substrate with different positions of electrodes. As shown in the results, all gas sensor samples exhibited a good response to collected male human breath samples of various races, which were Malay, Chinese, Indian, and Bumiputera from Sarawak. The best gas sensor for males were OG-T(G) and OG-T(K) with sensitivity, $S=1.10415$, and $S=1.01629$. Lastly, based on the comparison results, the fastest response time and recovery time for males were 0.52s and 13s, respectively.

Acknowledgement

This research was funded by Universiti Teknikal Malaysia Melaka (UTeM).

References

- [1] Wilson, Alphus D., and Manuela Baietto. "Advances in electronic-nose technologies developed for biomedical applications." *Sensors* 11, no. 1 (2011): 1105-1176. <https://doi.org/10.3390/s110101105>
- [2] Pavlou, A. K., and A. P. F. Turner. "Sniffing out the truth: clinical diagnosis using the electronic nose." (2000): 99-112. <https://doi.org/10.1515/CCLM.2000.016>
- [3] Berna, Amalia Z., and Audrey R. Odom John. "Breath metabolites to diagnose infection." *Clinical chemistry* 68, no. 1 (2022): 43-51. <https://doi.org/10.1093/clinchem/hvab218>
- [4] Das, Sagnik, and Mrinal Pal. "Non-invasive monitoring of human health by exhaled breath analysis: A comprehensive review." *Journal of The Electrochemical Society* 167, no. 3 (2020): 037562. <https://doi.org/10.1149/1945-7111/ab67a6>
- [5] Wallace, M. Ariel Geer, and Joachim D. Pleil. "Evolution of clinical and environmental health applications of exhaled breath research: Review of methods and instrumentation for gas-phase, condensate, and aerosols." *Analytica Chimica Acta* 1024 (2018): 18-38. <https://doi.org/10.1016/j.aca.2018.01.069>
- [6] Vasilescu, Alina, Borys Hrinchenko, Greg M. Swain, and Serban F. Peteu. "Exhaled breath biomarker sensing." *Biosensors and Bioelectronics* 182 (2021): 113193. <https://doi.org/10.1016/j.bios.2021.113193>
- [7] de Oliveira, Luciana Fontes, Celia Mallafre-Muro, Jordi Giner, Lidia Perea, Oriol Sibila, Antonio Pardo, and Santiago Marco. "Breath analysis using electronic nose and gas chromatography-mass spectrometry: A pilot study on bronchial infections in bronchiectasis." *Clinica Chimica Acta* 526 (2022): 6-13. <https://doi.org/10.1016/j.cca.2021.12.019>
- [8] Lubes, Giuseppe, and Mohammad Goodarzi. "GC-MS based metabolomics used for the identification of cancer volatile organic compounds as biomarkers." *Journal of pharmaceutical and biomedical analysis* 147 (2018): 313-322. <https://doi.org/10.1016/j.jpba.2017.07.013>
- [9] Majchrzak, Tomasz, Wojciech Wojnowski, Martyna Lubinska-Szczygeł, Anna Rózańska, Jacek Namieśnik, and Tomasz Dymerski. "PTR-MS and GC-MS as complementary techniques for analysis of volatiles: A tutorial review." *Analytica chimica acta* 1035 (2018): 1-13. <https://doi.org/10.1016/j.aca.2018.06.056>
- [10] Li, Baozhong, Xue Zou, Hongmei Wang, Yan Lu, Chengyin Shen, and Yannan Chu. "Standardization study of expiratory conditions for on-line breath testing by proton transfer reaction mass spectrometry." *Analytical biochemistry* 581 (2019): 113344. <https://doi.org/10.1016/j.ab.2019.113344>
- [11] Olivenza-León, David, Chris A. Mayhew, and Ramón González-Méndez. "Proton transfer reaction mass spectrometry investigations of phthalate esters via direct headspace sampling." *International Journal of Mass Spectrometry* 461 (2021): 116497. <https://doi.org/10.1016/j.ijms.2020.116497>
- [12] Saasa, Valentine, Thomas Malwela, Mervyn Beukes, Matlou Mokgotho, Chaun-Pu Liu, and Bonex Mwakikunga. "Sensing technologies for detection of acetone in human breath for diabetes diagnosis and monitoring." *Diagnostics* 8, no. 1 (2018): 12. <https://doi.org/10.3390/diagnostics8010012>
- [13] Španěl, Patrik, and David Smith. "Quantification of volatile metabolites in exhaled breath by selected ion flow tube mass spectrometry, SIFT-MS." *Clinical Mass Spectrometry* 16 (2020): 18-24. <https://doi.org/10.1016/j.clinms.2020.02.001>
- [14] Hryniuk, Alexa, and Brian M. Ross. "Detection of acetone and isoprene in human breath using a combination of thermal desorption and selected ion flow tube mass spectrometry." *International Journal of Mass Spectrometry* 285, no. 1-2 (2009): 26-30. <https://doi.org/10.1016/j.ijms.2009.02.027>

- [15] Saasa, Valentine, Thomas Malwela, Mervyn Beukes, Matlou Mokgotho, Chaun-Pu Liu, and Bonex Mwakikunga. "Sensing technologies for detection of acetone in human breath for diabetes diagnosis and monitoring." *Diagnostics* 8, no. 1 (2018): 12. <https://doi.org/10.3390/diagnostics8010012>
- [16] Wang, Weiran, Hengjie Su, Yuxiang Wu, Teng Zhou, and Ting Li. "Biosensing and biomedical applications of graphene: A review of current progress and future prospect." *Journal of The Electrochemical Society* 166, no. 6 (2019): B505. <https://doi.org/10.1149/2.1231906jes>
- [17] MOHD CHACHULI, Siti Amaniah, Yap PEI YEUAN, Omer COBAN, NH SHAMSUDIN, and M. Idzdihar IDRIS. "Investigation of Graphene Gas Sensor at Different Substrates for Acetone Detection." *Przegląd Elektrotechniczny* 99, no. 3 (2023).
- [18] Chachuli, Siti, Muhammad Noor, Ömer ÇOBAN, Nur Shamsudin, and Muhammad Idris. "Characteristic of graphene-based thick film gas sensor for ethanol and acetone vapor detection at room temperature." *INDONESIAN JOURNAL OF ELECTRICAL ENGINEERING AND COMPUTER SCIENCE* 32 (2023). <https://doi.org/10.11591/ijeecs.v32.i3.pp1384-1391>
- [19] Shoala, Tahsin. "Carbon nanostructures: Detection, controlling plant diseases and mycotoxins." In *Carbon Nanomaterials for Agri-Food and Environmental Applications*, pp. 261-277. Elsevier, 2020. <https://doi.org/10.1016/B978-0-12-819786-8.00013-X>
- [20] Ismail, Nur'Afini, Kamyar Shamel, Roshafima Rasit Ali, Siti Nur Amalina Mohamad Sukri, and Eleen Dayana Mohamed Isa. "Copper/graphene based materials nanocomposites and their antibacterial study: A mini review." *Journal of Research in Nanoscience and Nanotechnology* 1, no. 1 (2021): 44-52. <https://doi.org/10.37934/jrnn.1.1.4452>
- [21] Rashid, Nur Nadhirah Mohamad, Harith Ahmad, Mohammad Faizal Ismail, Siti Nur Fatin Zuikafly, Nur Azmah Nordin, Tsuyoshi Koga, Wira Jazair Yahya, Hafizal Yahaya, and Fauzan Ahmad. "Passively Q-Switched Thulium-Holmium Doped Fibre Laser with Electrochemical Exfoliation Graphene in Chitin Based Passive Saturable Absorber." *Journal of Advanced Research in Micro and Nano Engineering* 11, no. 1 (2023): 1-14. <https://doi.org/10.37934/armne.11.1.114>
- [22] How, Heoy Geok, Yeoh Jun Jie Jason, Yew Heng Teoh, and Hun Guan Chuah. "Investigation of tribological properties of graphene nanoplatelets in synthetic oil." *Journal of Advanced Research in Fluid Mechanics and Thermal Sciences* 96, no. 1 (2022): 115-126. <https://doi.org/10.37934/arfmts.96.1.115126>
- [23] Idumah, Christopher Igwe. "Design, development, and drug delivery applications of graphene polymeric nanocomposites and bionanocomposites." *Emergent Materials* 6, no. 3 (2023): 777-807. <https://doi.org/10.1007/s42247-023-00465-4>
- [24] Tseng, Shih-Feng, Chia-Ho Liao, Wen-Tse Hsiao, and Tien-Li Chang. "Ultrafast laser direct writing of screen-printed graphene-based strain electrodes for sensing glass deformation." *Ceramics International* 47, no. 20 (2021): 29099-29108. <https://doi.org/10.1016/j.ceramint.2021.07.071>
- [25] Hu, Qinhua, Anindya Nag, Yongzhao Xu, Tao Han, and Lijuan Zhang. "Use of graphene-based fabric sensors for monitoring human activities." *Sensors and Actuators A: Physical* 332 (2021): 113172. <https://doi.org/10.1016/j.sna.2021.113172>
- [26] Sigma Aldrich. "IR Spectrum Table." <https://www.sigmaaldrich.com/MY/en/technical-documents/technical-article/analytical-chemistry/photometry-and-reflectometry/ir-spectrum-table>
- [27] Das, Sagnik, Preeti Lata Mahapatra, Partha Pratim Mondal, Tanushri Das, Mrinal Pal, and Debdulal Saha. "A highly sensitive cobalt chromite thick film based trace acetone sensor with fast response and recovery times for the detection of diabetes from exhaled breath." *Materials Chemistry and Physics* 262 (2021): 124291. <https://doi.org/10.1016/j.matchemphys.2021.124291>
- [28] Zhai, Wei, Xinyu Li, Quanjun Xia, Pengfei Zhan, Jianwei Xu, Guoqiang Zheng, Kun Dai, Zhicheng Zhang, Chuntai Liu, and Changyu Shen. "Multi-functional and flexible helical fiber sensor for micro-deformation detection, temperature sensing and ammonia gas monitoring." *Composites Part B: Engineering* 211 (2021): 108621. <https://doi.org/10.1016/j.compositesb.2021.108621>
- [29] Zhai, Wei, Chunfeng Wang, Shuo Wang, Jiannan Li, Yi Zhao, Pengfei Zhan, Kun Dai, Guoqiang Zheng, Chuntai Liu, and Changyu Shen. "Ultra-stretchable and multifunctional wearable electronics for superior electromagnetic interference shielding, electrical therapy and biomotion monitoring." *Journal of Materials Chemistry A* 9, no. 11 (2021): 7238-7247. <https://doi.org/10.1039/D0TA10991F>
- [30] Venkatachalam, Srisaran, M. Depriester, A. Hadj Sahraoui, Bruno Capoen, M. R. Ammar, and D. Hourlier. "Thermal conductivity of Kapton-derived carbon." *Carbon* 114 (2017): 134-140. <https://doi.org/10.1016/j.carbon.2016.11.072>
- [31] Cui, Xiaoyun, Deepa Bhatt, Fuad Khoshnaw, David A. Hutt, and Paul P. Conway. "Glass as a substrate for high density electrical interconnect." In *2008 10th Electronics Packaging Technology Conference*, pp. 12-17. IEEE, 2008. <https://doi.org/10.1109/EPTC.2008.4763405>

- [32] Zaccaro, Andrea, Andrea Piarulli, Marco Laurino, Erika Garbella, Danilo Menicucci, Bruno Neri, and Angelo Gemignani. "How breath-control can change your life: a systematic review on psycho-physiological correlates of slow breathing." *Frontiers in human neuroscience* 12 (2018): 409421. <https://doi.org/10.3389/fnhum.2018.00353>